Materials Science Forum Vols. 467-470 (2004) pp. 551-556
online at http://www.scientific.net

Recrystallization in Deformed and Heat Treated PET Polymer Sheets

D. Raabe[1] and N. Chen[2]

[1] Max-Planck-Institut für Eisenforschung, Max-Planck-Str. 1, 40237 Düsseldorf, Germany

[2] Engineering Division, Colorado School of Mines, Golden, CO 80401, USA

Keywords: deformation, texture, decrystallization, amorphization, x-ray, cellular automaton, PET, PP, crystallization, spherulite, growth, semi-crystalline

Abstract. This is a study on texture, decrystallization, and recrystallization in rolled and heat treated semi–crystalline polymers. Experiments were conducted using wide angle Debye-Scherrer-type X–ray diffraction. Changes in crystallinity were quantitatively monitored as a function of strain and annealing time. It was observed that crystallinity drastically drops during deformation in PET. We suggest that amorphization (decrystallization) is a deformation mechanism which acts as an alternative to crystallographic slip depending on the orientation of the nanocrystalline lamellae. Heat treatment leads to the recrystallization of amorphous PET material and to an enhancement of the original texture of the deformed crystals observed before the heat treatment. We explain this phenomenon in terms of oriented nucleation where amorphous material crystallizes alongside existing crystalline lamellae.

Introduction

The properties of semi-crystalline thermoplastic polymers such as polyethylene terephthalate (PET) depend on their crystalline volume fraction [1,2] and on the crystallographic orientation distribution (texture) [3,4] of its nanocrystalline lamellae. Both properties change during deformation [3] and heat treatment [1,2]. Two processes play an essential role in this context, namely, decrystallization (strain-induced solid-state amorphization) during deformation and recrystallization during subsequent heat treatment [1-4]. In order to understand the relationship between these two processes and the reorientation of crystallites during deformation and heat treatment we present in this work a *quantitative* approach to the joint investigation of texture and crystallinity in semi-crystalline PET. In particular we address the following questions:

Semi–crystalline polymers consist of spherulites which contain nanocrystalline lamellae in an amorphous matrix. Various micromechanical mechanisms are conceivable for a crystal to reorient during deformation. One possibility is that crystals rotate due to the plastic spin arising from crystallographic shear. Another option is that crystals rotate due to skew-symmetric boundary conditions exerted by mechanical gradients in their amorphous neighborhood. A third possible mechanism is the strain-induced decrystallization of the nanocrystals and their dynamic recrystallization with a new orientation (pretended reorientation). By quantitatively monitoring orientational changes of the crystalline lamellae during mechanical loading we hope to elucidate the governing mechanism of texture formation during deformation.

It is obvious that the mechanisms of strain-induced amorphization and thermally-induced static recrystallization of amorphous material are closely connected to the texture. As far as strain-induced decrystallization is concerned it is likely that crystals which have an unfavorable orientation for crystallographic shear may instead undergo structural disintegration as a mode of deformation. As far as the recrystallization texture is concerned it is known that the material which was rendered amorphous during deformation can subsequently recrystallize (relax) upon heat treatment. However, it is still unclear whether this process follows an oriented nucleation or a growth selection mechanisms. We believe that quantitative texture analysis in conjunction with the determination of the change in crystallinity can help to identify the orientation dependence of both mechanisms.

Experimental

The study was conducted on commercial semi-crystalline PET and PP sheets with an initial thickness of 10mm. The samples were rolled at room temperature. Each pass exerted a thickness reduction of about 0.1 mm. Crystallographic textures were measured on samples deformed to different true (logarithmic) strain levels. Samples with a true strain of 1.2 were heat treated at 373K and 473K, respectively, for different annealing times ranging from 2s to 160 minutes.

The texture measurements were carried out on an X–ray texture goniometer with an area detector. The measurements were carried out using $Cr_{K\alpha 1}$ radiation at a tube current of 40mA and a voltage of 40kV. For reconstructing complete Debye–Scherrer diagrams covering the entire pole sphere we collected 162 frames for each sample condition (integration time for one frame was 100s). From the Debye–Scherrer frames $\{100\}$, $\{1\bar{1}0\}$, and $\{010\}$ pole figures were reconstructed. The sample symmetry was orthorhombic and the crystal symmetry triclinic. The parameters of the unit cell are a=4.5 Å, b=5.9 Å, c=107 Å, α=100°, β=118°, and γ=112° [5]. The pole figures served as input for the calculation of the ODF using the texture component method in the formulation of Helming et al. [6]. The method uses sets of Gauss- or Lorentz-shaped spherical functions with individual height and full width at half maximum as a measure for the strength and scatter of a texture component. The ODF is approximated by a superposition of such functions [see 6].

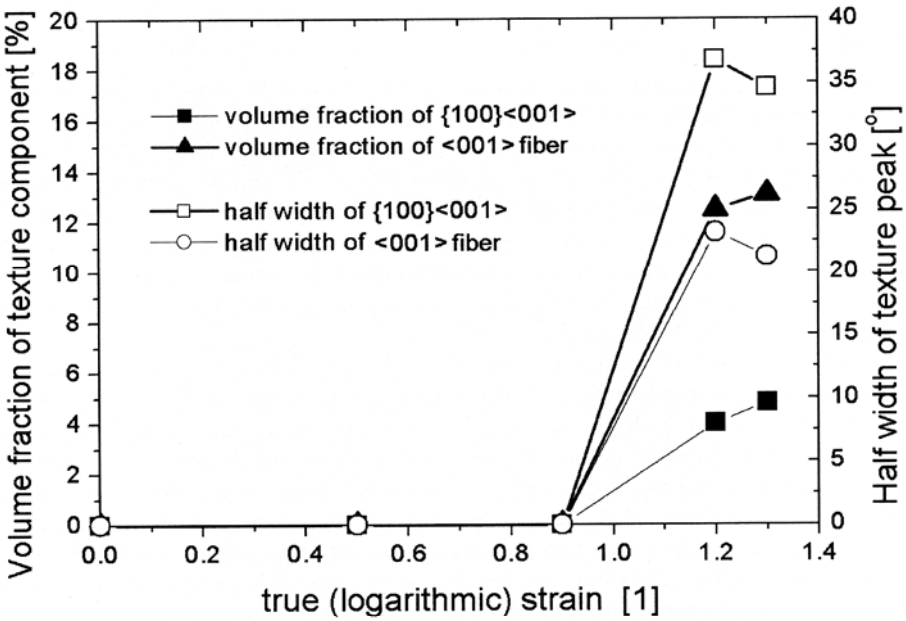

Fig. 1 Development of the orientation distribution of the nanocrystalline lamellae in terms of the volume fractions and half widths of the two main texture components during deformation in PET. Pole figure inversion and subsequent texture analysis was conducted using the texture component method in the formulation of Helming et al. [6].

Experimental Results and Interpretation

Fig. 1 shows the evolution of the two main orientations during deformation, namely, of the triclinic {100}<001> component and of the triclinic <001> fiber component. The texture becomes stronger with increasing deformation. At a strain of 1.2 the {100}<001> component is characterized by a volume fraction of 4% and a Gaussian scatter of 36.96° (full width at half maximum). The fiber component occupies 12.5% volume fraction at 23.2° scatter.

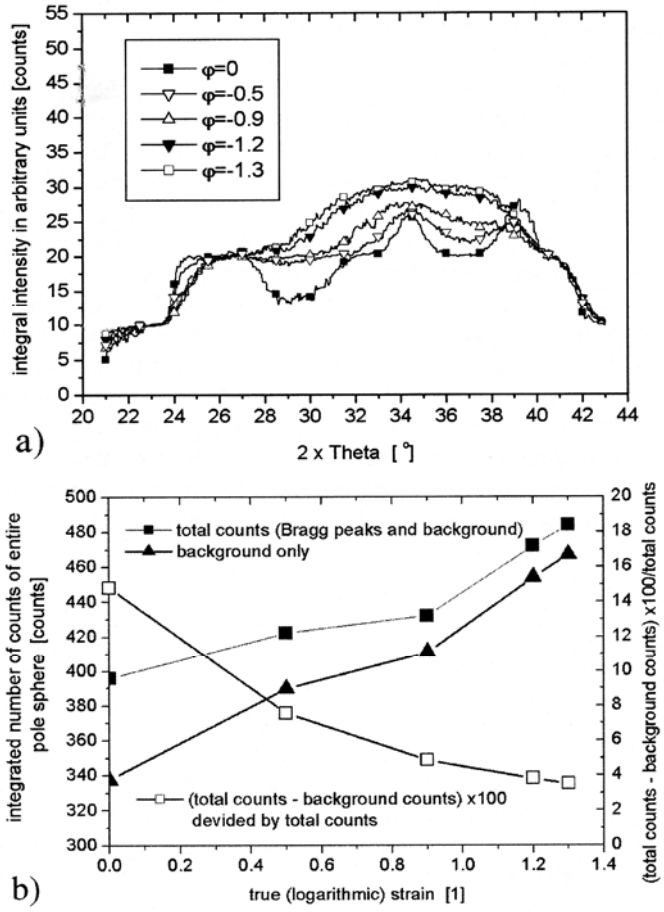

Fig. 2 a) Integrated wide angle X–ray scans as a function of strain (integration of 162 Debye–Scherrer frames for each sample condition).
b) Integrated number of total counts (full squares), integrated number of background counts (full triangles), and relative change (in %) in the number of all counts minus the background counts as a function of deformation. The latter curve (open squares) is a measure for the relative change in crystallinity during rolling.

Reviews on the deformation mechanisms in semi-crystalline polymers were published by Haudin [7], Lotz and Wittmann [8], Crist [9,10], and by the group of Bartczak, Argon, and Cohen [11-13]. It was found that the crystalline portions of PE, Nylon, and PET mainly deform by crystallographic shear on {hk0} planes (crystallographic chain slip). The weak van der Waals bonding between

neighboring covalently bonded molecule chains allows for glide between such chains in either the <001> chain axis direction or transverse direction <uv0>. Symmetry considerations show that crystallographic slip in PET does not provide five independent shear systems as required for a closed yield surface, owing to the low (triclinic) symmetry of PET crystals. This means that the von Mises compatibility criterion is violated when assuming crystallographic slip as the only mode of plastic deformation. Based on these observations [7-13] and on our own predictions obtained by a Sachs-type deformation model with three types of potential slip systems we find that the {100}<001> texture component and also some part of the <001> texture fiber can be explained in terms of the activation of the {100}<001> slip system.

Fig. 2 shows the strong decrease in crystallinity during deformation. This measurement is based on the integration of 162 separate Debye–Scherrer frames covering the entire pole sphere, i.e. the data are quantitative. Fig. 2b shows the corresponding relative change in the number of all X-ray counts minus the background signal as a function of deformation. The data reveal a drop in the relative diffraction signal with increasing total strain from ~15% to ~3%. This translates to a change in the crystalline volume from ~85% (undeformed) to ~17% at a strain of 1.2. A possible explanation of this gradual amorphization is that sheared crystalline lamellae break apart into sets of crystalline blocks which contain severe lattice defects [8,9]. This process is often referred to as mechanical melting. Such a mechanism would entail substantial broadening of the Bragg cones before their total disappearance. This was indeed confirmed by the Debye-Scherrer diagrams which show that there is no abrupt transition between the crystalline and the amorphous phase. The large Bragg peak broadening can be regarded as a proof of an intermediate or semi-amorphous ordering state between the crystalline and the completely amorphous phase. Such a model of a block-type arrangement of small crystalline portions with intermediate chain tangles was earlier suggested by Bellare [12] for PE. In this case the authors assumed that the crystal lamellae break apart into stacks of crystalline fragments during straining similar as in the present case.

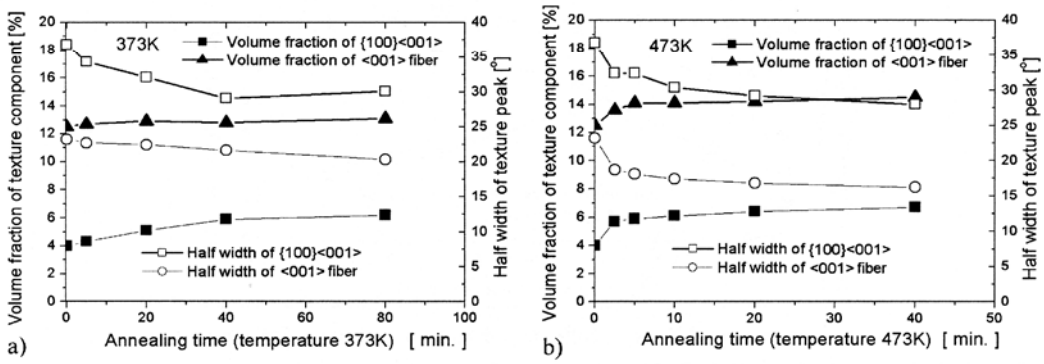

Fig. 3 Texture changes during heat treatment. a) 373K, b) 473K.

This strain-induced decrystallization is accompanied by the evolution of a pronounced deformation texture of the remaining crystals. This means that amorphization is a texture-dependent process. In order to reconcile these two observations (amorphization of crystals versus reorientation of crystals) we suggest that in particular those crystals which cannot deform by crystallographic (100)[001] chain slip, due to their vanishing Schmid factor, are prone to undergo amorphization. This means that texture evolution and strain-induced decrystallization are simply linked via the orientation factor of the crystals. Hence, amorphization can be regarded as a microscopic deformation mode in semi-crystalline PET. It is an isotropic rather than a anisotropic contribution to

the yield locus. We suggest that the easiest mode of deformation for a crystalline lamella is the shear on a (100)[001] chain slip system. When stressed along a direction which does not favor activation of this system, however, the respective crystal undergoes decrystallization as an alternative mode of deformation. In other words if the local stress in a PET crystal reaches the yield surface in any direction other than that prescribed by single slip the lamella is decrystallized. Since our data (Fig. 1) show the evolution of a deformation texture on the basis of chain slip it may be concluded that the critical stress for the activation of strain-induced amorphization is larger than that for the activation of (100)[001] chain slip.

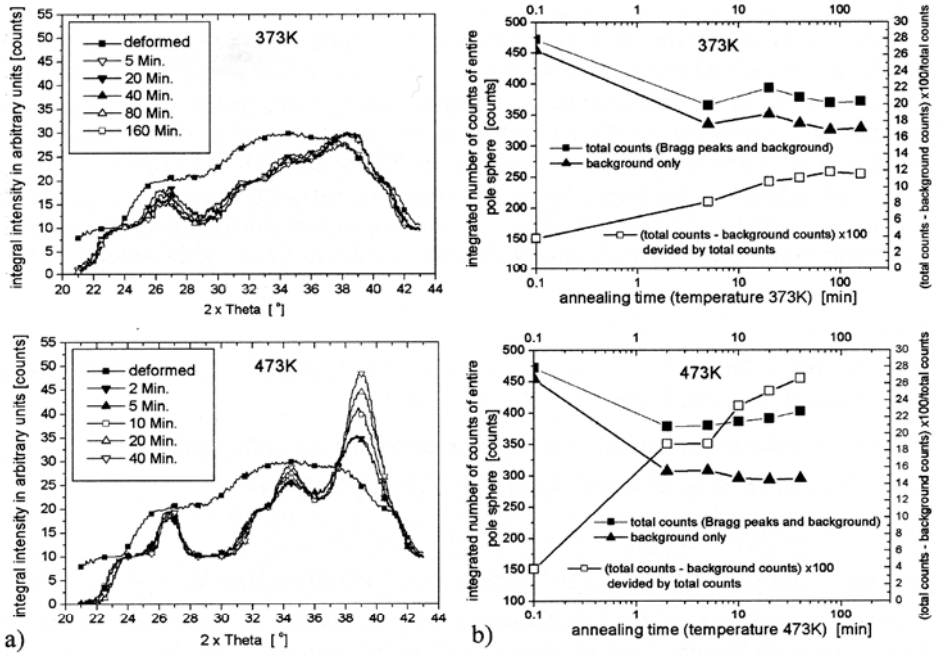

Fig. 4 a) Integrated wide angle X–ray scans (deformed PET, true strain: 1.2) during heat treatment (373K, 473K). Integration over all Debye–Scherrer frames measured for one sample condition. b) Integrated number of all counts (full squares), integrated number of background counts (full triangles), and relative change (in %) in the number of all counts minus the background counts. The latter curve (open squares) is a measure for the relative change in crystallinity during rolling.

The last topic is the evolution of texture and crystallinity during heat treatment. Fig. 3 shows the changes in volume fraction and half width of the two main orientation components during heat treatment. At 373K the half width of the two components decreases as a function of the annealing time. The volume fraction of the <001> fiber component remains almost constant while the {100}<001> component slightly increases during heat treatment. At 473K the volume fraction of both texture components increases and their half width decreases during annealing. The kinetics of texture sharpening are much faster at 473K than at 373K.

The heat treatment (373K, 473K) of strained specimens (true strain:1.2) leads to the recrystallization of amorphous material and to an enhancement of the original deformation texture (Fig. 4). This applies in particular to 473K (Fig. 4b) where the data show a strong change of the relative diffraction signal as a function of time during isothermal heat treatment. The texture evolution reveals that recrystallization does not lead to new crystalline orientations, but to a

sharpening of the preceding deformation texture. This leads us to the conclusion that recrystallization works in the present case by an oriented nucleation or respectively relaxation mechanism where the amorphous material aligns along existing crystalline lamellae or fragmented lamellae blocks which were not decrystallized during rolling. By relaxation we mean that it is conceivable that the observed recrystallization process might occur via the re-alignment of the small crystalline blocks which were suggested as a typical microstructure of rolled and broken lamellae. This argumentation is supported by the strong sharpening of the Bragg cones upon heat treatment.

Summary

We presented a study on texture, amorphization, and recrystallization in semi–crystalline polymers (PET, PP). It was found that amorphization proceeds as a function of strain. We suggest that such decrystallization acts as a deformation mechanism which takes place as an alternative to crystallographic slip depending on the orientation of the polymer crystals. Heat treatment leads to the recrystallization of amorphous material and to an enhancement of the original texture of the crystals observed before heat treatment. We explain this observation in terms of oriented nucleation where amorphous material crystallizes alongside existing crystalline lamellae. Recrystallization kinetics and spherulite sizes were qualitatively simulated by use of a cellular automaton.

References

[1] Asano, T., Balta Calleja, F. J., Flores, A., Tanigaki, M., Mina, M. F., Sawatari, C., Itagaki, H., Takahashi, H. & Hatta, I., Polymer 40 (1999) 6475

[2] Bedia, E., Murakami, S., Kitade, T. & Kohjiya, S. Polymer 42 (2001) 7299

[3] Bellare, A., Cohen, R. E. & Argon, A. S., Polymer 34 (1993) 1393

[4] Göschel, U., Deutscher, K. & Abetz V., Polymer 37 (1996) 1

[5] Encyclopedia of Polymer Science and Engineering. 2nd edition New York:Wiley, 1985

[6] Helming, K., Schwarzer, R. A., Rauschenbach, B., Geier, S., Leiss, B., Wenk, H. R., Ullemeier, K. & Heinitz, J., Z. Metallkunde 85 (1994) 545

[7] Haudin JM, in B. Escaig and C. G'Sell (eds.), Plastic Deformation of Amorphous and Semi-Crystalline Materials, Les Editions de Physique, Les Ulis, 1982, page 291

[8] Lotz B. & Wittmann J. C., Structure of Polymer Single Crystals, in: Structure and Properties of Polymers, 1993, Vol. ed. E.L. Thomas, Vol. 12 of Materials Science and Technology, ed. by R. W. Cahn, P. Haasen, E. J. Kramer, page 79

[9] Crist, B., Plastic Deformation of Polymers, in: Structure and Properties of Polymers, 1993, Vol. ed. E.L. Thomas, Vol. 12 of Materials Science and Technology, ed. by R. W. Cahn, P. Haasen, E. J. Kramer, Chapter 10, page 427

[10] Crist, B., Semicrystalline Polymers: Plastic Deformation, in: Encyclopedia of Materials: *Science and Technology*, Volume 9, K. H. J. Buschow et al., eds., Elsevier, New York, 2001, page 8427

[11] Lee, B. J., Argon, A. S., Parks, D. M., Ahzi, S. & Bartczak, Z., Polymer 34 (1993) 3555

[12] Bellare, A., Cohen, R. E. & Argon, A. S., Polymer 34 (1993) 1393

[13] Bartczak, Z., Argon, A. S. & Cohen, R. E., Polymer 35 (1994) 3427